

COMPUTER DETERMINATION OF HOM DAMPING for a PROTOTYPE JLC  
ACCELERATOR CAVITY and a PROTOTYPE B FACTORY CAVITY\*

Norman M. Kroll†  
University of California, San Diego,  
Department of Physics- 0319 La Jolla, CA 92093-0319  
and  
Stanford Linear Accelerator Center, Stanford University, Stanford, CA. 94309

Robert Rimmer‡  
Lawrence Berkeley Laboratory,  
UCB, Berkeley, CA. 94720

## Abstract

In this paper we describe the determination of the properties of the above referenced cavities with particular emphasis on the damping of the higher order modes (HOM). Because mode frequency spectra were determined for a large number of shorted waveguide lengths, rather complete analyses are possible. Phase frequency plots have proved to be an invaluable aid in sorting out overlapping resonances and separating cavity resonances from waveguide resonances. Algorithms for the determination of the parameters of several resonances simultaneously have been developed. Determinations of  $Q$  from multiresonance analyses are compared to those from single resonance analyses, and the changes are typically found to be small.

## 1. INTRODUCTION

The damping of higher order modes in accelerator cavities has been a subject of extensive study for many years. The primary technique employed has been to couple the energy out through wave guides to be terminated in matched loads. Computer programs such as MAFIA (as in this paper) have been extensively employed to assist in the design of such structures. To obtain values of the  $Q_{ext}$  and the shifted resonant frequencies due to the wave guide loading, it has been necessary to develop special analysis techniques to be applied to the results obtained from a program such as MAFIA. The methods of Kroll-Yu<sup>1</sup> (KY) and Kroll-Lin<sup>2</sup> (KL, or KYL when referring to them collectively) are examples of such techniques and will be employed for the two problems which we discuss in this paper. The thrust of KYL was aimed towards minimizing the number of computer runs needed. The two examples discussed here are, however, considerably more complex than those discussed in those papers, and the rather large number used here have permitted a more complete overall analysis of the mode spectrum. Also, since we are still acquiring experience with these methods, the larger "data sample" is very useful for providing validation.

A problem which we have experienced in applying KYL has been the separation of waveguide resonances from cavity resonances. One deals here with the spectrum of a lossless coupled cavity waveguide system, and any run at a particular waveguide length will produce a series of resonances, some cavity associated, some waveguide associated, and some, when the two occur at neighboring frequencies, strongly coupled. When the waveguide coupling is not too strong, these cases can be readily distinguished by inspection of field plots. Current interest, however, centers about the strongly coupled case where this method has not always been convincing. We have found phase-frequency plots to be of great assistance in sorting out this problem.

The phase of a given computer determined mode at a particular waveguide length is given by

$$\phi = 2\pi L/\lambda_g$$

As the length is varied each mode traces out a section of a phase-frequency curve. As pointed out by KY each such section is displaced by a multiple of  $\pi$  from a single universal curve that applies to all of the modes. The designation "phase-frequency plot" is intended to refer to that single universal curve. An example is

\*Works supported by Department of Energy contracts AS03-89ER40527†, AC03-76SF00515†, and AC03-76SF00098#.

provided by Fig. 1. It is based on data reported by Higo et. al at the LINAC 90 conference<sup>3</sup>. We were provided with a list of the lowest seven modes arising from MAFIA runs at twelve different waveguide lengths. The quantity  $n\pi$  was subtracted from the phase of the  $n$ 'th mode at each length and the entire set of 84 points plotted. As is apparent from Fig. 1, the points do indeed trace out a smooth curve. The high density of points in the low frequency portion of the curve results from the high degree of overlap which results from the  $n\pi$  shifts. The smallness of the scatter is an indication of the high quality of the computer output. The cavity resonances are associated with the steeper portions of the curve, and as we shall discuss later, the low frequency portion is indicative of overlapping resonances. The presence of these overlapping resonances has been the motivation for the development of multiresonance fitting procedures. Both single mode propagation and a unique symmetry relation between the fields in the two outputs has been assumed in the above discussion. These were assured by the boundary conditions applied in the MAFIA calculations.

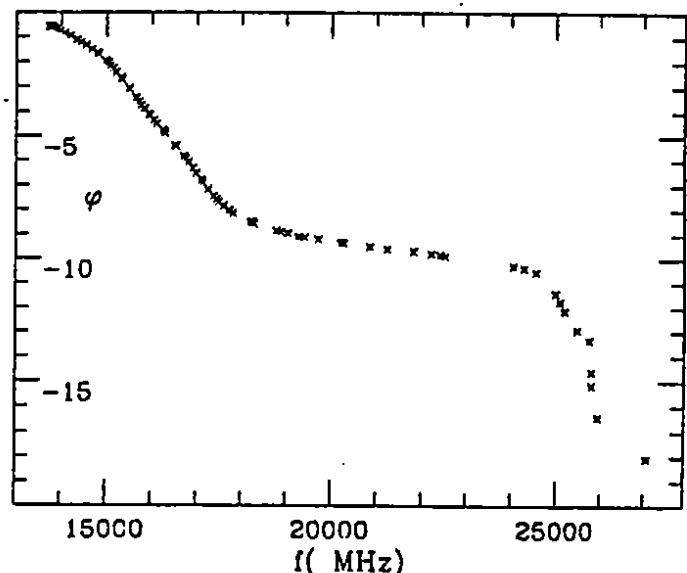


Fig. 1 Phase frequency plot for JLC prototype cavity.

## 2. THE JLC CAVITY

The KYL methods are based upon the following representation of the phase-frequency relation:

$$\phi(\omega) = \sum_i \arctan \left( \frac{v_i}{\omega - u_i} \right) - \chi(\omega)$$

$$\chi(\omega) = \chi_0 + \omega\chi'$$

For each mode,  $u/2v$  is the  $Q$  value and  $u$  the resonant frequency. The branches of the arctangents are to be chosen so as to obtain a smooth curve. The function  $\chi$  is intended to represent the effect of resonances not taken into account explicitly. If one ignores  $\chi$ , it is apparent that as the frequency passes through a resonance the phase decreases by  $\pi$ . If all resonances occurring within a given

frequency interval are recognized and included explicitly in eq. (1), then  $\chi$  may be presumed to be due to resonances outside the interval and therefore to vary by substantially less than  $\pi$  over the same interval. Thus we do not consider a "feature" in the phase-frequency plot to correspond to a resonance unless a phase change of  $\pi$  is involved, and strongly overlapping resonances produce phase changes which are multiples of  $\pi$ .

Applying these considerations to Fig. 1, we conclude that the region below 18000 MHz contains three overlapping resonances, the region 18000-24000 MHz is resonance free, and the region 24000-26000 MHz contains two resonances. The isolated point above 26000 suggests an additional resonance, but because of inadequate supporting information we ignore it in our analysis. We determined resonance parameters for the three low frequency and two high frequency parameters separately. To obtain parameters for the low frequency resonances we chose eight more or less evenly spaced data points between 15340 and 18236 MHz, and determined the six resonance parameters and two  $\chi$  parameters so that the theoretical curve passed through the eight selected points. The results of this procedure are shown in Fig. 2. The resultant fit is seen to be excellent, and the theoretical curve fits the data accurately until the high frequency resonances are approached. Attempts to fit the data with only two resonances failed and showed clearly that the

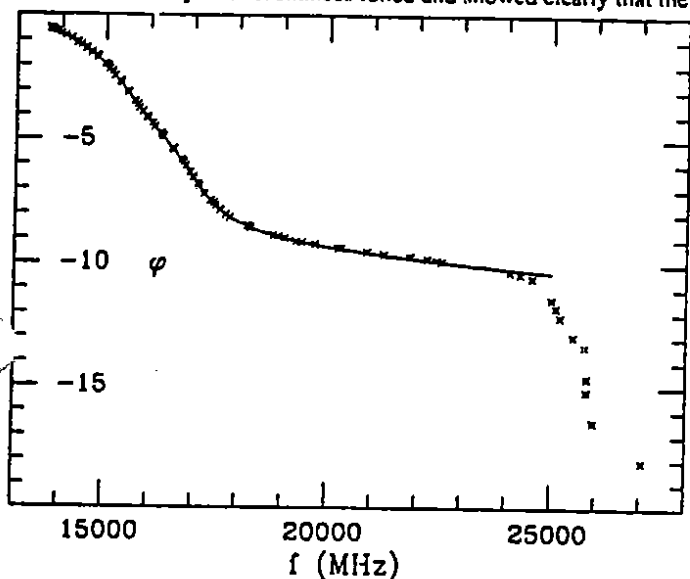


Fig. 2 Three resonance eight point fit for the low frequency resonances.

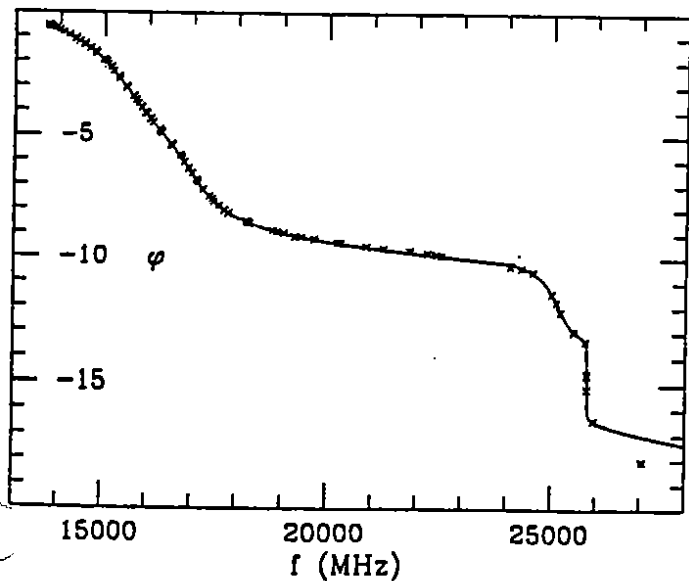


Fig. 3 Composite plot of the low frequency fit of Fig. 2 with a two resonance six point fit to the high frequency resonances. The break point is at 24100 MHz.

phase span in the resonance region combined with the slope of the resonance free region is inconsistent with the assumption that only two resonances are involved. For the high frequency resonances we selected six points in the range 25006 to 25956 MHz and determined four resonance parameters and two  $\chi$  parameters so that the theoretical curve passed through the six selected points. A composite curve containing both fits is shown in Fig. 3. The break between the two representations occurs at  $\sim 24100$  MHz where the two curves cross. Frequencies and  $Q$  values that yielded Fig. 3 are shown in Table I. The figures in parentheses are those obtained from single resonance four parameter fits carried out with data points selected from the neighborhood of the resonance as determined by visual inspection of Fig. 1. Mode 2 is not discernible in this way and attempts to find it with the four point method after its position had been determined were not successful. Nevertheless the results show that the four point method can give quite reliable results even in the presence of severe overlap. It appears that the free slope parameter does a quite effective job of taking account of the effect of omitted resonances on the  $Q$  values.

Table I. Frequencies and  $Q$ 's for the JLC Cavity

Mode Number	Frequency (MHz)	$Q$
1	15375 (15552)	10.9 (12.0)
2	16077	7.1
3	17048 (16927)	14.8 (13.5)
4	25121 (25138)	43.1 (42.0)
5	25814 (25814)	-1000 (-1000)

We have not identified the modes because we have not seen the associated field plots. Fig. 1 of ref. 3 plus the symmetry imposed in the MAFIA calculations suggest  $TM_{110}-\pi$  for mode 1 and  $TE_{111}-0$  for mode 2 or 3. We suspect that the other of these two modes is associated with the radial slot in the disk.

### 3. THE PROTOTYPE B FACTORY CAVITY

The cavity referred to in the heading above consists of a pill box with three waveguides mounted symmetrically on one end, emerging perpendicular to the end, and with the wide dimension perpendicular to the radius. In addition it includes a cylindrical section of smaller radius intended to represent the beam pipe, symmetrically disposed on the two ends and terminated with a short. A computer simulation of half the cavity is shown in Fig. 4. It is a B factory prototype only in the context of a study of higher order mode damping.

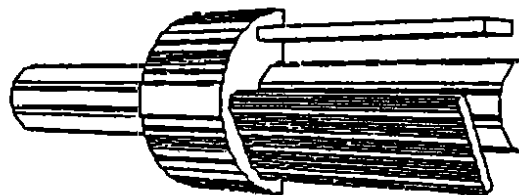


Fig. 4 MAFIA simulation of the prototype B factory cavity used for the MAFIA computations.

Because the cavity is symmetric under  $120^\circ$  rotation about the beam axis, its modes can be characterized by an  $m=-1, m=0$ , or  $m=1$  symmetry index corresponding to the lowest Fourier component in the azimuthal Fourier expansion of the fields. The  $m=\pm 1$  modes are degenerate, but because only half the cavity is modeled only a single linear combination of this pair appears. Thus we can analyze the  $m=0$  and  $m=1$  modes separately.

MAFIA calculations were carried out for 14 different lengths of waveguide, beginning with zero. The results of the calculation are summarized in Fig. 5. Connecting lines have been drawn which preserve the mode order of  $m=1$  and  $m=0$  modes separately. Identification was based upon the fact that fields at the end of the waveguide should be equal for the  $m=0$  case and in the ratio -1 to 2 for the  $m=1$  case (the -1 refers to the amplitude in the full width waveguide). Because the computer mesh does not accurately reflect

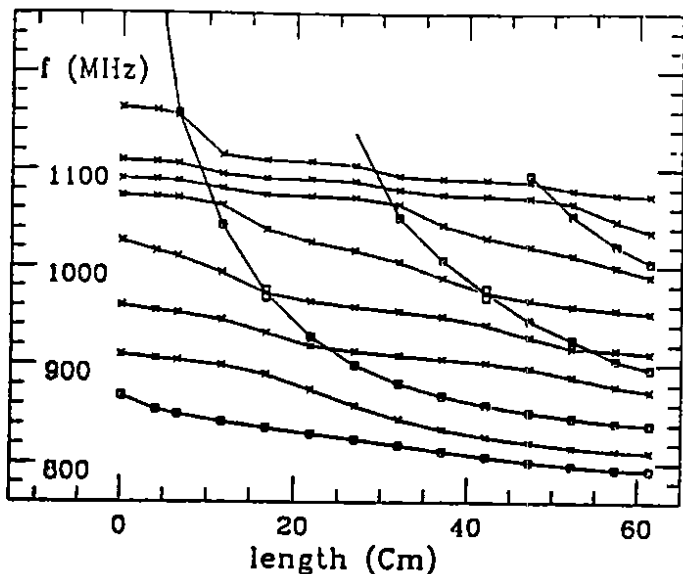


Fig. 5 MAFIA computed mode spectra of the Prototype B factory cavity shown as a function of the length of the shorted waveguides. Connecting lines join points belonging to the same symmetry class.  
 $m=0$  square points.  $m=1$  x points.

the symmetry of the physical structure, these relations are satisfied only approximately, and large deviation occurs at the crossing points. The  $n\pi$  displacement procedure is applied to the  $m=0$  and  $m=1$  sequences separately, and the phase-frequency curves illustrated in Fig. 6 emerge. The squares mark  $m=0$  and the x's  $m=1$ . The four "star" points are from the crossing regions and have ambiguous symmetry. Both points appear on each curve. These points were avoided in carrying out frequency- $Q$  determinations. The figure also contains points from a calculation carried out at length 61.29cm with a magnetic boundary condition imposed at the waveguide ends. These fall on the universal curves if their phase is displaced by an extra  $\pi/2$ .

The  $m=0$  curve exhibits a maximum at the low frequency end instead of the usual monotonic decrease. This is due to a mode trapping phenomenon which has plagued the application of waveguide damping. The mode involved here is the  $TM_{011}$ . It has a frequency of 868.36 MHz for the closed cavity, well above the waveguide cutoff of 786.86. As the waveguides emerge from the cavity end and lengthen, the frequency of the mode is pulled down and eventually falls below the guide cutoff frequency. When this happens the phase-frequency plot is guaranteed to exhibit a maximum as a function of frequency. (The reality of this phenomenon has been confirmed with an analytically solvable model.) The mode did not actually fall below cutoff at the largest length (61.29cm). However, the appearance of the maximum is considered to be the indication that it will eventually do so. Replacing the electric boundary condition with a magnetic one at the waveguide end has an effect similar to increasing the length, and such a calculation was performed to see whether it would exhibit an extra trapped mode. Indeed such a mode was found at 773.87 MHz, which we take to be a confirmation of the above. Apart from the trapped mode, the  $m=0$  curve shows only one resonance, a detrapped and low  $Q$  counterpart of the trapped  $TM_{011}$  mode. The determination of the resonance parameters of this mode is degraded by the fact that the KY phase-frequency formula does not include the trapping phenomenon, so that the  $Q$  determination appears to be uncertain up to a factor two or so.

The  $m=1$  phase-frequency curve is of the expected form and clearly shows the seven lowest waveguide damped  $m=1$  modes. Four parameter single resonance fits have been carried out using both the KY and, where adequate data was available, the KL method. The phase-frequency plot identifies appropriate regions for the selection of data points for fitting and enables one to avoid the study of waveguide resonances. The two methods are found to be in excellent agreement except for the low  $Q$   $TM_{011}$  mode. As mentioned before, we consider this to be due to the fact that the

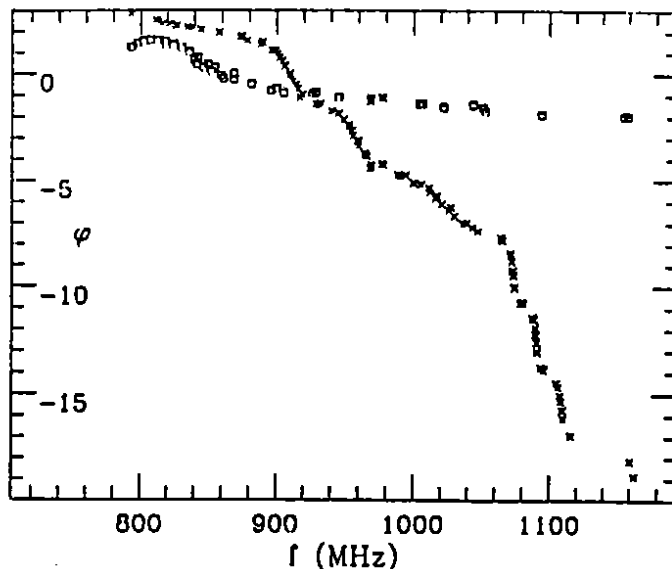


Fig. 6 Phase-frequency plot for the prototype B factory cavity.  
 $m=0$  square points.  $m=1$  x points.  
 ambiguous (plotted twice) star points.

phase-frequency formula does not include the trapping phenomenon. These results are summarized in Table II. The waveguide loaded frequencies  $F_L$  for the trapped modes are taken directly from the MAFIA results.

Table II. Frequencies and  $Q$ 's for the Prototype B Factory Cavity

Mode type	$F_0$ (MHz)	$F_L(KY)$ (MHz)	$F_L(KL)$ (MHz)	$Q(KY)$	$Q(KL)$
$TM_{010}$	617.17		610.94		trapped
$TE_{111}$	711.61		708.00		trapped
$TM_{011}$	868.36		<773.87		trapped
$TM_{011}$		841-842	840-845	15-17	24-35
$TM_{110}$	909.58	906.7	906.7	55	56
$TE_{210}$	959.92	956.9	956.6	56	55
$TM_{111}$	1027.22	1021.3	1021.4	32	31
$TM_{112}$	1073.44	1073.0	1073.7	338	336
$TM_{113}$	1090.53	1090.0	1090.0	401	411
$TM_{114}$	1109.39	1108.6	1107.5	300	318
unknown ( $m=1$ )	1163.15	1162.0		333	

The  $TM_{11n}$  modes above 1070 MHz are associated with the sudden opening of the beam pipe to propagation in the  $TE_{11}$  waveguide mode (cutoff at 1064 MHz). The bulk of the stored energy as well as the extra nodes are in the beam pipe for all three. An experimental investigation of this cavity has been carried out by Voelker et al<sup>4</sup>. Absorbers were placed in the beam pipe so that agreement with computed  $Q$ 's of the "beam pipe" modes is not expected. Otherwise reasonable agreement was obtained.

We thank T. Higo and M. Takao for providing us with the MAFIA generated data for the JLC cavity, and X-T. Lin for assistance with the graphics.

#### REFERENCES

1. N. Kroll and D. YU, Part. Acc. 34 p. 231 (1990)
2. N. Kroll and X. Lin, Proc. 1990 Linac Conf. Albuquerque, NM, June 10-14 (1990) p. 238
3. T. Higo, M. Takao, M. Suetake, K. Kubo, and K. Takata, Proc. 1990 Linac Conf. Albuquerque, NM, June 10-14 (1990) p. 147. We undertook the analysis of this cavity at the request of T. Higo.
4. F. Voelker, G. Lambertson, and R. Rimmer; IEEE Part. Acc. Conf., San Francisco, CA. May 6-9 (1991) Abs. IIRA22.